npj | Quantum Materials

www.nature.com/npjquantmats

PERSPECTIVE OPEN

Check for updates

$MnBi_2Te_4$-family intrinsic magnetic topological materials

Ke He[1]✉

$MnBi_2Te_4$ and its derivative compounds have received focused research interests recently for their inherent magnetic order and the rich, robust and tunable topological phases hosted in them. Here, I briefly introduce $MnBi_2Te_4$-family intrinsic magnetic topological materials—the electronic and magnetic properties, the topological phase diagrams and the research progress made on them in the past years. I try to present a simple picture to understand their rich electronic, magnetic and topological properties, and a concise guide to engineer them for intended topological phases and the quantum anomalous Hall effect at higher temperature.

npj Quantum Materials (2020)5:90 ; https://doi.org/10.1038/s41535-020-00291-5

QUANTUM ANOMALOUS HALL EFFECT

"We call simple systems that perform robustly in complex situations elegant". The quote by Jesse Schell in his book *The Art of Game Design*, accidently, captures the essence of topological states of matter—an elegant way to preserve quantum characteristics of materials plagued by disorders and imperfections[1,2]. As wonderfully illustrated in the quantum anomalous Hall (QAH) effect, clean quantized plateaus of Hall resistance and dissipationless electron transport can be observed in centimeter-sized magnetically doped topological insulator (TI) samples, with strong disorder induced by randomly scattered magnetic impurities[3]. However, a flaw remains in the elegance of the QAH effect in these materials—the extremely low temperature required to exhibit the quantized transport properties. The first observation of the QAH effect was made at 30 mK, and the temperature was elevated barely to 1 K after years of effort[4,5].

INTRINSIC MAGNETIC TOPOLOGICAL INSULATOR $MNBI_2TE_4$

In a first-principles calculation work by E. V. Chulkov's group from San Sebastián, Spain in 2017, it was found that if a MnTe bilayer is artificially inserted into the first quintuple layer of Bi_2Te_3, constructing a $MnBi_2Te_4$ septuple layer (SL; Fig. 1a), a rather large magnetically induced energy gap (up to 77 meV, much larger than the <1 meV gap in usual magnetically doped TIs) is opened at the topological surface states (TSSs), which promises a robust QAH state[6]. The $MnBi_2Te_4$ capping layer, then considered as a ferromagnetic insulator (FMI) by the authors, somehow allows the TSSs of Bi_2Te_3 to pervade it and strongly interact with the Mn atoms (termed as "magnetic extension" by the authors), which leads to the huge magnetic gap.

Little was known on the material at that time because, as a metastable phase, its single-crystal samples are rather difficult to prepare[7]. At the end of 2017, our group first obtained thin films of $MnBi_2Te_4$ with molecular beam epitaxy and checked their electronic structure with in situ angle-resolved photoemission spectroscopy (K.H., talk in Zhengzhou University International Forum for Young Scholars on December 17, 2017)[8]. Amazingly, the $MnBi_2Te_4$ films exhibit archetypical Dirac-cone-shaped bands around Fermi level—a characteristic of a 3D TI. If $MnBi_2Te_4$ is indeed a 3D TI (not considering its magnetism), the mysterious "magnetic extension" in $MnBi_2Te_4$-covered Bi_2Te_3 becomes straightforward to understand. 3D TIs have a special property: put two 3D TIs together, you get one 3D TI, with the TSSs appearing only at the surface of the whole system[9]. Naturally, the TSSs will "extend" to the $MnBi_2Te_4$ capping layer on Bi_2Te_3.

Indeed, according to the calculation results, the energy bands of $MnBi_2Te_4$ near Fermi level are dominated by the *p* bands of Bi and Te, which contribute to the TI property[10–12]. The hybridization between the *p* bands and the *d* bands of Mn atoms, several electron volts away from Fermi level, is weak enough to retain the TI characteristic, but strong enough to induce a significant magnetic gap at the TSSs when the magnetic order is built (Fig. 1b, c). We call it an intrinsic magnetic TI because the magnetism comes from the compound itself, rather than from magnetic dopants or neighboring layers, which is crucial for the enough strong *p*–*d* hybridization inducing the large magnetic gap.

$MnBi_2Te_4$ has a A-type antiferromagnetic (AFM) structure: every ferromagnetic (FM) SL, with out-of-plane easy magnetic axis, is weakly antiferromagnetically coupled with neighboring SLs. The interplay between the magnetic structure and the topological nontrivial bands endows the material with rich topological phases[10–12]. Actually, one can easily understand the topological phases of $MnBi_2Te_4$ and other similar compounds $MnBi_{2n}Te_{3n+1}$ ($n \geq 1$) based on the theoretical topological phase diagrams given by A. A. Burkov and L. Balents in 2011 by considering the materials as superlattices between MnTe (FMI) and Bi_2Te_3 (TI) layers of different thicknesses[13].

When the magnetic order vanishes at an enough high temperature, a FMI/TI superlattice degenerates into a normal insulator (NI)/TI superlattice. Its topological phase, as shown in Fig. 2a, depends on the competition between the hybridizations of the TSSs from the same TI layers (Δ_S) and from neighboring TI layers (Δ_D). Clearly, a superlattice with thinner NI layers (larger Δ_D) and thicker TI layers (smaller Δ_S) tends to be a TI, while that with thicker NI layers (smaller Δ_D) and thinner TI layers (larger Δ_S) tends to be a NI. When the FMI layers recover their ferromagnetism and are coupled antiferromagnetically (A-type AFM structure), the phase diagram is similar except that the TI phase is replaced by the AFM TI (Fig. 2b), which is exactly the ground state of $MnBi_2Te_4$. AFM TI is a TI protected by the combined time-reversal and translation symmetry, and possesses gapless TSSs only at surfaces parallel to the magnetization axis[14].

In $MnBi_2Te_4$ thin films, the A-type AFM structure makes the magnetization vectors of the top and bottom SLs parallel for the odd-number SL thickness, and antiparallel for the even-number SL thickness. In the former case, the top and bottom surfaces have topologically different surface states, and are thus bounded by a

[1]State Key Laboratory of Low-Dimensional Quantum Physics, Department of Physics, Tsinghua University, 100084 Beijing, China. ✉email: kehe@tsinghua.edu.cn

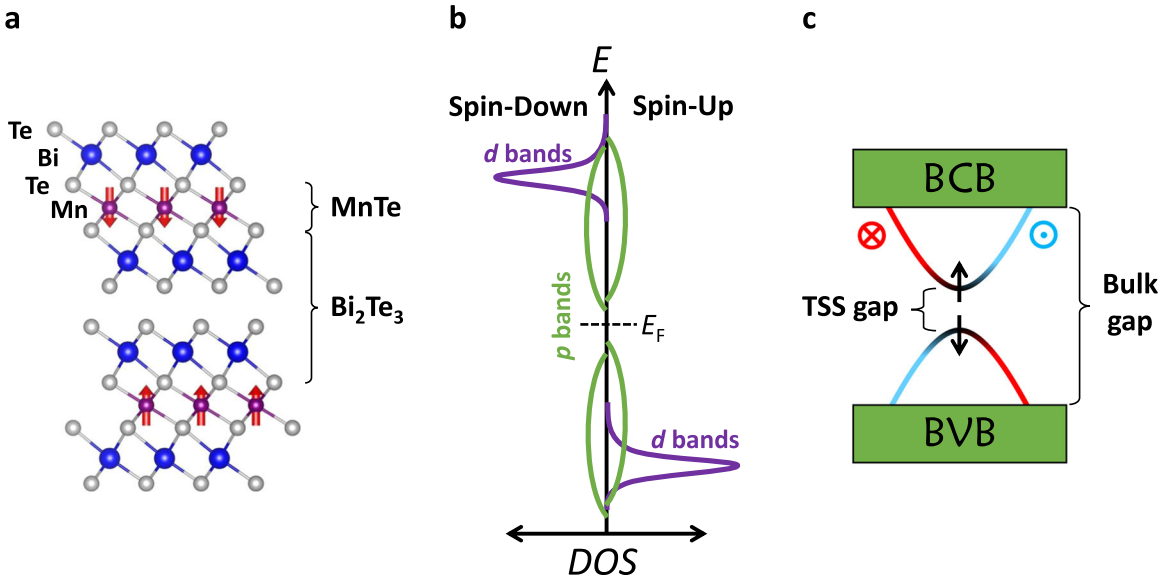

Fig. 1 Lattice and electronic structures of $MnBi_2Te_4$. a Schematic lattice structure of $MnBi_2Te_4$. **b** Schematic bulk energy band structure of $MnBi_2Te_4$. **c** Schematic topological surface states (TSSs) of $MnBi_2Te_4$.

gapless chiral edge channel at the film edge (Fig. 2e), which makes a QAH insulator with Chern number (C) of unity. In the latter case, the two surfaces are the same in their topological properties, and the film is an axion insulator characterized by the topological magnetoelectric effect (Fig. 2d)[11,15].

If the FMI layers of a FMI/TI superlattice are magnetized in the same direction, its topological phase is determined by the competitions among Δ_S, Δ_D, and the magnetic gap of the TSSs (m), as shown in the phase diagram in Fig. 2c (ref. [13]). When Δ_S is large compared with m, while Δ_D is small, the superlattice is a usual FMI. When Δ_D is large compared with m, while Δ_S is small, the superlattice is a FMI that becomes a TI when the FM order is lost above the Curie temperature. The thin films of such a phase will exhibit $C = 1$ QAH effect, similar to magnetically doped TI Cr-doped $(Bi,Sb)_2Te_3$. The phase is denoted by "FMTI", since FM order and TI phase do not exist at the same time though in the same material[3,16]. When both Δ_S and Δ_D are large compared with m, the superlattice enters the magnetic Weyl semimetal (WSM) phase. Its thin films can show the QAH effect with Chern number (the number of chiral edge channels) depending on the film thickness (Fig. 2f, g)[17,18]. When Δ_S and Δ_D are both small compared with m, the TSSs are decoupled with each other, and the superlattice can be considered as many parallel and isolated QAH systems which is denoted by QAH multilayer (ML)[19]. The rich topological phases found in $MnBi_2Te_4$-family materials can be understood and engineered based on the phase diagrams.

RESEARCH PROGRESS ON $MNBI_2TE_4$

Rapid and exciting experimental progress has been made in $MnBi_2Te_4$-family materials in the past years, constructing one of the hottest topics in condensed matter physics recently[8,20–36]. Single-crystal samples of $MnBi_2Te_4$-family materials have been successfully prepared by several groups[20–27]. The A-type AFM structure has been demonstrated with SQUID measurements and directly observed with magnetic force microscopy[28,29]. A magnetic field of several Tesla is enough to overcome the weak AFM interlayer coupling and make $MnBi_2Te_4$ FM, as shown by the stepped hysteresis loops characterizing a van der Waals magnetic material[8]. The spectroscopic results of $MnBi_2Te_4$ family materials, however, are controversial[8,20–23,30–33]. There is still no consensus on whether the observed TSSs are gapped or gapless and why they are insensitive to temperature.

Above all, quantized transport properties have been observed in $MnBi_2Te_4$ thin flakes exfoliated from $MnBi_2Te_4$ single crystals by several groups above 1.5 K, higher than in usual magnetically doped TI samples[34–36]. In odd-SL thick flakes, Yuanbo Zhang and Xianhui Chen's group observed quantized plateaus of the Hall resistance, as well as diminishing longitudinal resistance, both in the AFM configuration around zero magnetic field and in the FM configuration at magnetic field of several Tesla[35]. Yayu Wang and Jinsong Zhang's group observed the topological phase transition between axion insulator and QAH insulator in even-SL thick $MnBi_2Te_4$ flakes, as the magnetic configuration is changed between AFM to FM by magnetic field[35]. Jian Wang's group observed $C = 2$ plateau (at magnetic field of several Tesla) at relatively thick $MnBi_2Te_4$ flakes, which provides a strong evidence for the magnetic WSM phase in FM $MnBi_2Te_4$. Furthermore, in some samples, nearly quantized Hall resistance (90.4% h/e^2) plateau is observed up to 45 K, even higher than the Néel temperature of $MnBi_2Te_4$ (25 K)[36]. The seemingly counter-intuitive observation can be understood with the 2D magnetism of the material. In such a 2D magnetic system, according to the Mermin–Wagner theorem, the magnetic ordering temperature is determined by the magnetic anisotropy energy which suppresses magnetic fluctuations. An external magnetic field enhances the effective magnetic anisotropy energy, and can thus hold long-range FM order to higher temperature. The result implies that the QAH states in $MnBi_2Te_4$ are indeed quite robust and may exist at higher temperature, with a more efficient way to suppress the magnetic fluctuations.

The key to control the topological phases in $MnBi_2Te_4$-family compounds is to engineer their magnetic structures, especially the interlayer magnetic coupling (IMC). A recent theoretical work has revealed that the IMC of $MnBi_2Te_4$-family materials is essentially the superexchange interaction and follows the Goodenough–Kanamori rules[37,38]. It enables us to obtain the magnetic WSM phase with FM ground state, as well as other interesting topological phases by constructing heterostructures between different $MnBi_2Te_4$-family materials[37]. Different from the short-ranged superexchange coupling in ferrites (usually mediated by only one oxygen ion), the IMC of $MnBi_2Te_4$-family materials is significant even with the neighboring FM layers spaced by six nonmagnetic atoms and a

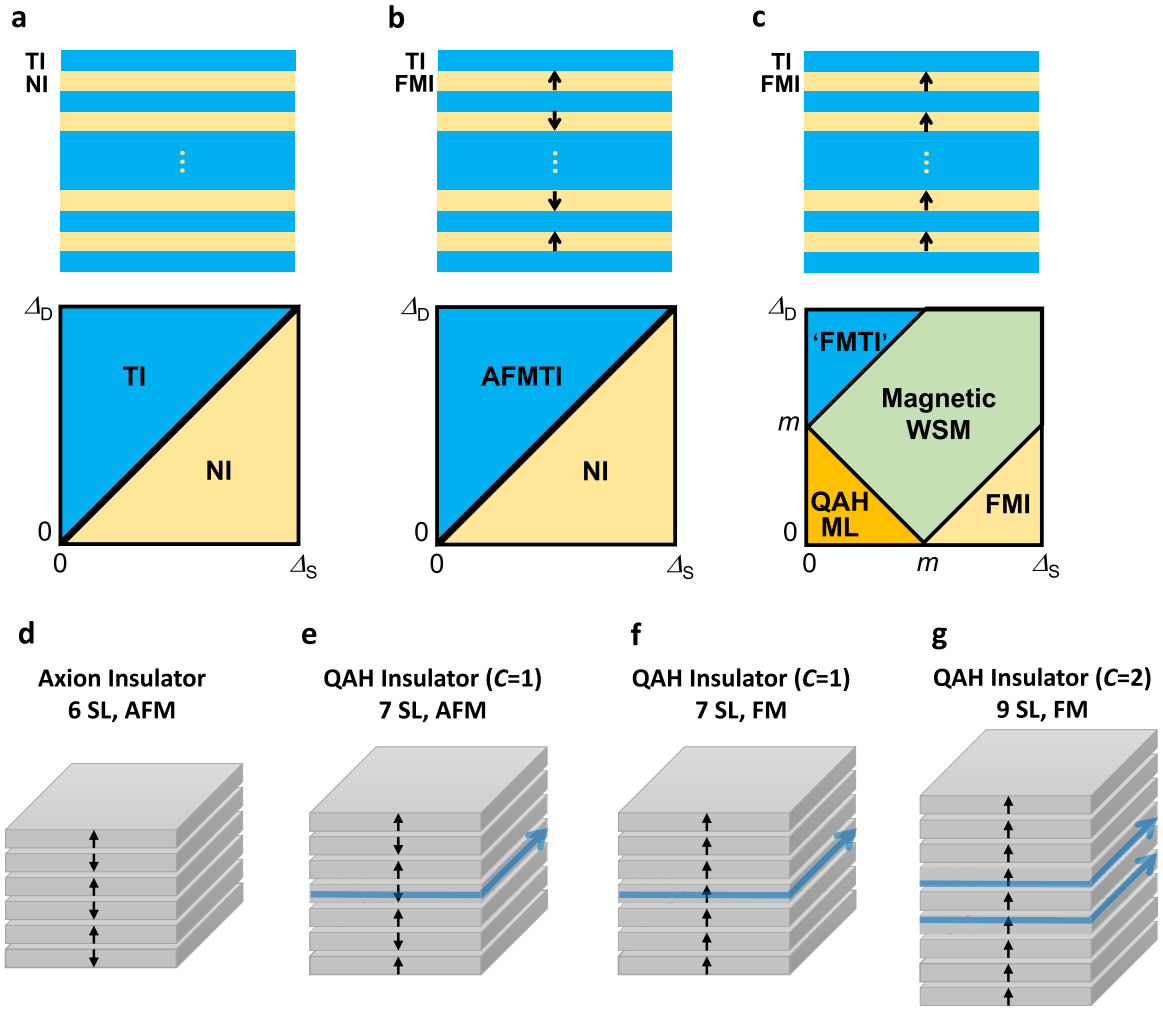

Fig. 2 Topological phases of $MnBi_2Te_4$-family materials. a–c Topological phase diagrams of NI/TI superlattice (**a**), FMI/TI superlattice in AFM configuration (**b**), and FMI/TI superlattice in FM configuration (**c**). **d–g** Schematic topological phases of $MnBi_2Te_4$ thin films or flakes in different thickness and magnetic configurations.

van der Waals gap, reaching 16.5 meV (~190 K) in $NiBi_2Te_4$. The super-long-ranged superexchange coupling is possible because Bi and Te atoms have similar electronegativities, and both possess rather delocalized *p* orbitals, which greatly facilitates electron hopping between them[37].

The result that IMC strength of van der Waals magnetic materials can far exceed the energy scale of liquid nitrogen temperature (77 K) indicates a way to achieve high temperature QAH effect in $MnBi_2Te_4$. Choosing an appropriate FMI neighboring layer that are strongly coupled with $MnBi_2Te_4$ may significantly suppress magnetic fluctuations in it, without needing external magnetic field[37,39]. The Curie temperature should be mainly determined by the IMC strength, which can exceed 77 K. Sandwiching a $MnBi_2Te_4$ film with two such FMI layers would thus lead to the QAH effect above the liquid nitrogen temperature.

CONCLUSION AND PROSPECTIVE

So, $MnBi_2Te_4$-family materials and heterostructures provide us a neat, simple, and versatile way to fuse topological energy bands with magnetic order, and unveil a feasible road map to push the occurring temperature of the QAH effect above 77 K. They may thus play a crucial role in achieving wide practical applications of the QAH effect, as well as other related quantum effects, opening up the gate toward a new concept electronics based on elegant topological quantum states.

Received: 30 August 2020; Accepted: 6 November 2020;
Published online: 07 December 2020

REFERENCES

1. Haldane, F. D. M. Nobel Lecture: topological quantum matter. *Rev. Mod. Phys.* **89**, 040502 (2017).
2. Wen, X. G. Colloquium: zoo of quantum-topological phases of matter. *Rev. Mod. Phys.* **89**, 041004 (2017).
3. Chang, C.-Z. et al. Experimental observation of the quantum anomalous Hall effect in a magnetic topological insulator. *Science* **340**, 167–170 (2013).
4. Mogi, M. et al. Magnetic modulation doping in topological insulators toward higher-temperature quantum anomalous Hall effect. *Appl. Phys. Lett.* **107**, 182401 (2015).
5. Ou, Y. et al. Enhancing the quantum anomalous Hall effect by magnetic codoping in a topological insulator. *Adv. Mater.* **30**, 1703062 (2018).
6. Otrokov, M. M. et al. Highly-ordered wide bandgap materials for quantized anomalous Hall and magnetoelectric effects. *2D Mater.* **4**, 025082 (2017).
7. Lee, D. S. et al. Crystal structure, properties and nanostructuring of a new layered chalcogenide semiconductor, Bi_2MnTe_4. *CrystEngComm* **15**, 5532–5538 (2013).
8. Gong, Y. et al. Experimental realization of an intrinsic magnetic topological insulator. *Chin. Phys. Lett.* **36**, 076801 (2019).

9. Chang, C. Z. et al. Band engineering of Dirac surface states in topological-insulator-based van der Waals heterostructures. *Phys. Rev. Lett.* **115**, 136801 (2015).
10. Li, J. et al. Intrinsic magnetic topological insulators in van der Waals layered $MnBi_2Te_4$-family materials. *Sci. Adv.* **5**, eaaw5685 (2019).
11. Zhang, D. et al. Topological axion states in the magnetic insulator $MnBi_2Te_4$ with the quantized magnetoelectric effect. *Phys. Rev. Lett.* **122**, 206401 (2019).
12. Otrokov, M. M. et al. Unique thickness-dependent properties of the van der waals interlayer antiferromagnet $MnBi_2Te_4$ films. *Phys. Rev. Lett.* **122**, 107202 (2019).
13. Burkov, A. A. & Balents, L. Weyl semimetal in a topological insulator multilayer. *Phys. Rev. Lett.* **107**, 127205 (2011).
14. Mong, R. S. K., Essin, A. M. & Moore, J. E. Antiferromagnetic topological insulators. *Phys. Rev. B* **81**, 245209 (2010).
15. Qi, X. L., Hughes, T. L. & Zhang, S. C. Topological field theory of time-reversal invariant insulators. *Phys. Rev. B* **78**, 195424 (2008).
16. Yu, R. et al. Quantized anomalous Hall Effect in magnetic topological insulators. *Science* **329**, 61–64 (2010).
17. Wan, X., Turner, A. M., Vishwanath, A. & Savrasov, S. Y. Topological semimetal and Fermi-arc surface states in the electronic structure of pyrochlore iridates. *Phys. Rev. B* **83**, 205101 (2011).
18. Xu, G., Weng, H., Wang, Z., Dai, X. & Fang, Z. Chern semimetal and the quantized anomalous Hall effect in $HgCr_2Se_4$. *Phys. Rev. Lett.* **107**, 186806 (2011).
19. Jiang, G. et al. Quantum anomalous Hall multilayers grown by molecular beam epitaxy. *Chin. Phys. Lett.* **35**, 076802 (2018).
20. Otrokov, M. M. et al. Prediction and observation of an antiferromagnetic topological insulator. *Nature* **576**, 416 (2019).
21. Rienks, E. D. L. et al. Large magnetic gap at the Dirac point in $Bi_2Te_3/MnBi_2Te_4$ heterostructures. *Nature* **576**, 423 (2019).
22. Lee, S. H. et al. Spin scattering and noncollinear spin structure-induced intrinsic anomalous Hall effect in antiferromagnetic topological insulator $MnBi_2Te_4$. *Phys. Rev. Res.* **1**, 012011 (2019).
23. Wu, J. et al. Natural van der Waals heterostructural single crystals with both magnetic and topological properties. *Sci. Adv.* **5**, eaax9989 (2019).
24. Cui, J. et al. Magnetic and transport properties in the magnetic topological insulators $MnBi_2Te_4(Bi_2Te_3)_n$ ($n = 1, 2$). *Phys. Rev. B* **99**, 155125 (2019).
25. Chen, B. et al. Intrinsic magnetic topological insulator phases in the Sb doped $MnBi_2Te_4$ bulks and thin flakes. *Nat. Commun.* **10**, 4469 (2019).
26. Yan, J.-Q. et al. Crystal growth and magnetic structure of $MnBi_2Te_4$. *Phys. Rev. Mater.* **3**, 064202 (2019).
27. Li, H. et al. Antiferromagnetic topological insulator $MnBi_2Te_4$: synthesis and magnetic properties. *Phys. Chem. Chem. Phys.* **22**, 556–563 (2020).
28. Sass, P. M. et al. Magnetic imaging of domain walls in the antiferromagnetic topological insulator $MnBi_2Te_4$. *Nano Lett.* **20**, 2609–2614 (2020).
29. Sass, P. M. et al. Robust A-type order and spin-flop transition on the surface of the antiferromagnetic topological insulator $MnBi_2Te_4$. *Phys. Rev. Lett.* **125**, 037201 (2020).
30. Hao, Y.-J. et al. Gapless surface Dirac cone in antiferromagnetic topological insulator $MnBi_2Te_4$. *Phys. Rev. X* **9**, 041038 (2019).
31. Li, H. et al. Dirac surface states in intrinsic magnetic topological insulators $EuSn_2As_2$ and $MnBi_{2n}Te_{3n+1}$. *Phys. Rev. X* **9**, 041039 (2019).
32. Chen, Y.-J. et al. Topological electronic structure and its temperature evolution in antiferromagnetic topological insulator $MnBi_2Te_4$. *Phys. Rev. X* **9**, 041040 (2019).
33. Yuan, Y. et al. Electronic states and magnetic response of $MnBi_2Te_4$ by scanning tunneling microscopy and spectroscopy. *Nano Lett.* **20**, 3271–3277 (2020).
34. Deng, Y. et al. Quantum anomalous Hall effect in intrinsic magnetic topological insulator $MnBi_2Te_4$. *Science* **367**, 895–900 (2020).
35. Liu, C. et al. Robust axion insulator and Chern insulator phases in a two-dimensional antiferromagnetic topological insulator. *Nat. Mater.* **19**, 522–527 (2020).
36. Ge, J. et al. High-Chern-number and high-temperature quantum Hall effect without Landau levels. *Natl Sci. Rev.* **7**, 1280–1287 (2020).
37. Li, Z. et al. Tunable interlayer magnetism and band topology in van der Waals heterostructures of $MnBi_2Te_4$-family materials. *Phys. Rev. B* **102**, 081107 (2020).
38. Goodenough, J. B. *Magnetism and the Chemical Bond* (Interscience (Wiley), New York, 1963).
39. Fu, H., Liu, C. X. & Yan, B. H. Exchange bias and quantum anomalous Hall effect in the $MnBi_2Te_4/CrI_3$ heterostructure. *Sci. Adv.* **6**, eaaz0948 (2020).

ACKNOWLEDGEMENTS

This work was supported by the National Natural Science Foundation of China (51661135024), the National Key Research and Development Program of China (2017YFA0303303), and the Beijing Advanced Innovation Center for Future Chip (ICFC).

AUTHOR CONTRIBUTIONS

K.H. conceived and wrote the paper.

COMPETING INTERESTS

The author declares no competing interests.

ADDITIONAL INFORMATION

Correspondence and requests for materials should be addressed to K.H.

Reprints and permission information is available at http://www.nature.com/reprints

Publisher's note Springer Nature remains neutral with regard to jurisdictional claims in published maps and institutional affiliations.